

Supplementary Information

Development of low-cost tissue paper-based chemosensor and demonstration for selective detection of Cu²⁺ and Hg²⁺ ions

Bharathkumar Thangaraj,^a Marimuthu Ponram,^a Suresh Ranganathan,^{b,c} Sambath Baskaran,^d Ravichandran Cingaram,^a Sathiyarayanan Kulathu Iyer,^e and Karthikeyan Natesan Sundaramurthy*^a

^aDepartment of Chemistry, Easwari Engineering College, Chennai 600 089, India.

^bCentre for Material Chemistry, Karpagam Academy of Higher Education, Coimbatore, India.

^cDepartment of Chemistry, Karpagam Academy of Higher Education, Coimbatore, India.

^dDepartment of Materials Science and Engineering, Korea Advanced Institute of Science and Technology (KAIST), Daejeon 34141, Republic of Korea.

^eSchool of Advanced Sciences, Vellore Institute of Technology (VIT), Vellore 632 014, India.

*Corresponding author: Email id: karthikeyan.ns12@gmail.com

Table of CONTENTS

Fig. S1. The ^1H NMR spectra of **intermediate 1**

Fig. S2. The ^{13}C NMR spectra of **intermediate 1**

Fig. S3. The HR-MS spectra of **intermediate 1**

Fig. S4. The ^1H NMR spectra of **DPICDT**

Fig. S5. The ^{13}C NMR spectra of **DPICDT**

Fig. S6. The HR-MS spectra of **DPICDT**

Fig. S7. Changes in fluorescence intensity of **DPICDT** in THF on the addition of DMSO.

Fig. S8. Job's plot for **DPICDT** Vs Cu^{2+} and Hg^{2+} in $\text{CH}_3\text{CN}:\text{H}_2\text{O}$ (8:2, v/v)

Fig. S9. The HR-MS spectra of **DPICDT-Cu²⁺**

Fig. S10. The HR-MS spectra of **DPICDT-Hg²⁺**

Fig. S11. B–H plot of the 1: 1 complex of probe **DPICDT** with Cu^{2+} and Hg^{2+} ions

Fig. S12. Linear plot of fluorescence intensity versus concentration of Cu^{2+} and Hg^{2+} ions

Fig. S13. FT-IR spectra of probe **DPICDT**, **DPICDT-Cu²⁺** and **DPICDT-Hg²⁺ (ClO₄)₂⁻**.

Fig. S14. AAS spectrum of **DPICDT** with Cu^{2+} and Hg^{2+}

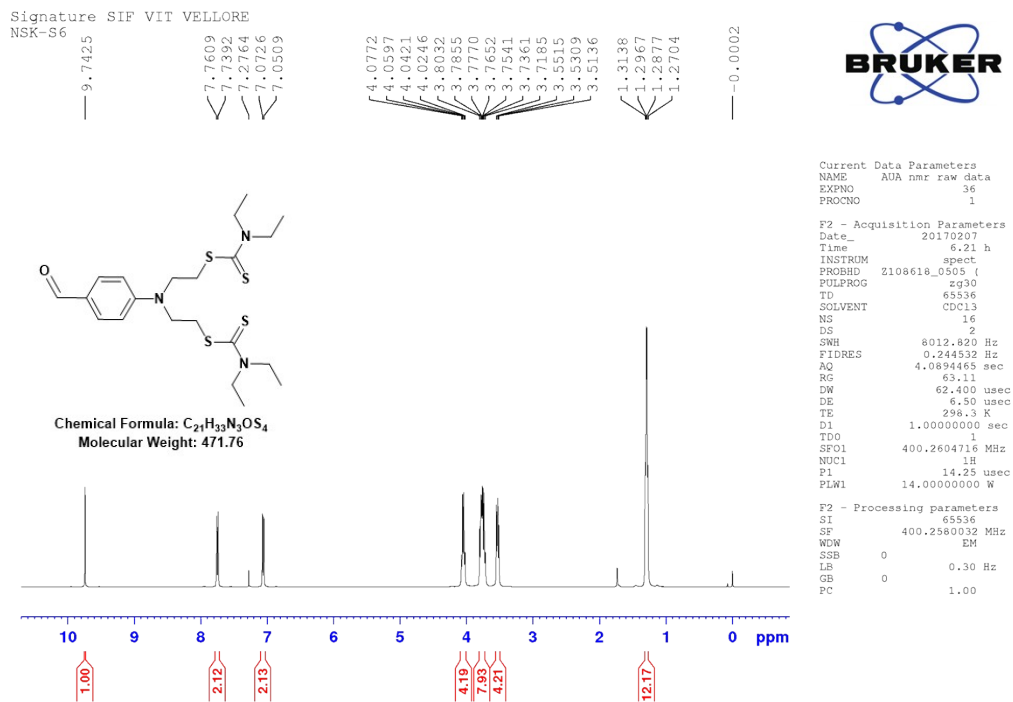


Fig.S1. The ^1H NMR spectra of intermediate 1

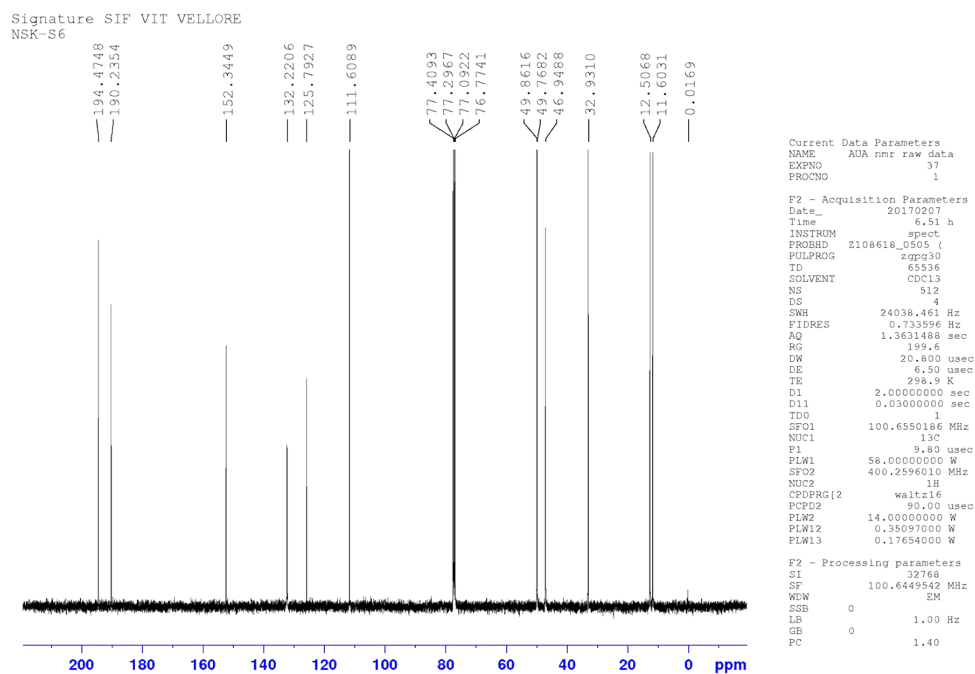


Fig.S2. The ^{13}C NMR spectra of intermediate 1

Spectra

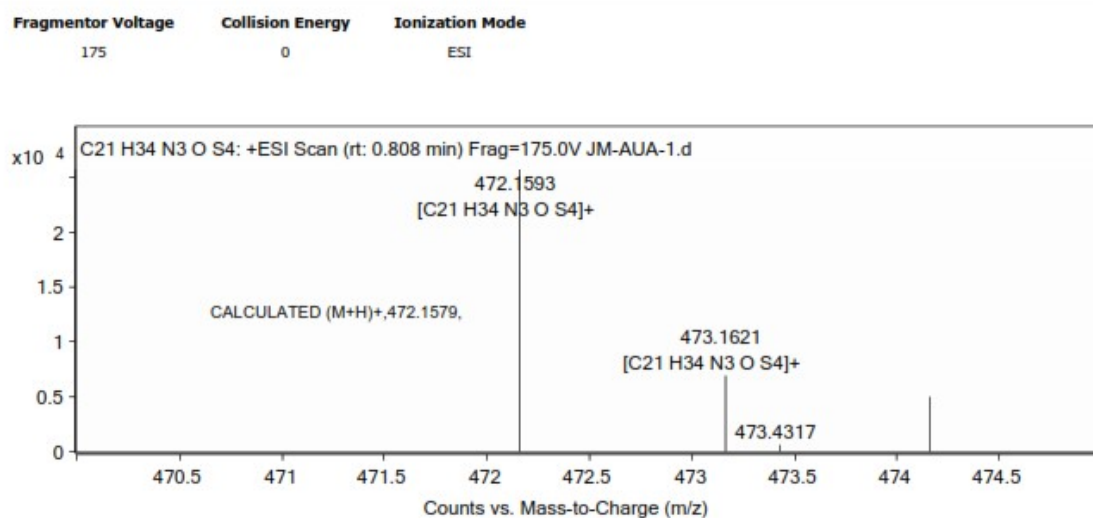


Fig.S3. The HR-MS spectra of intermediate 1.

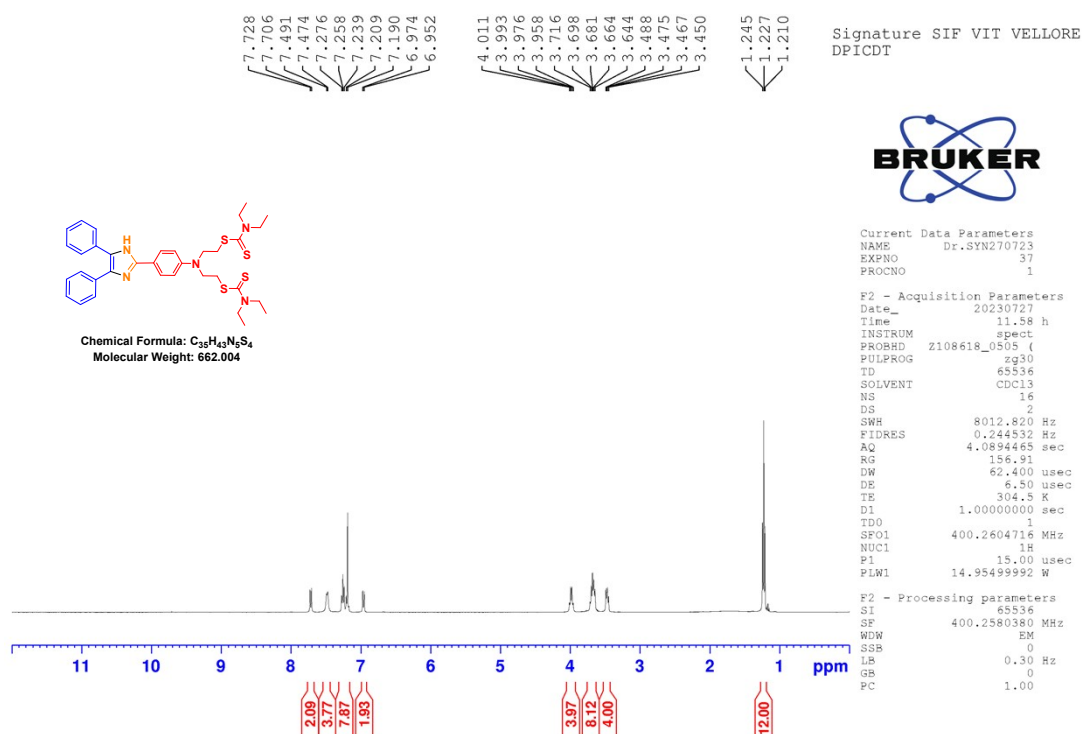


Fig.S4. The ^1H NMR spectra of DPICDT.

Signature SIF VIT VELLORE
BEN

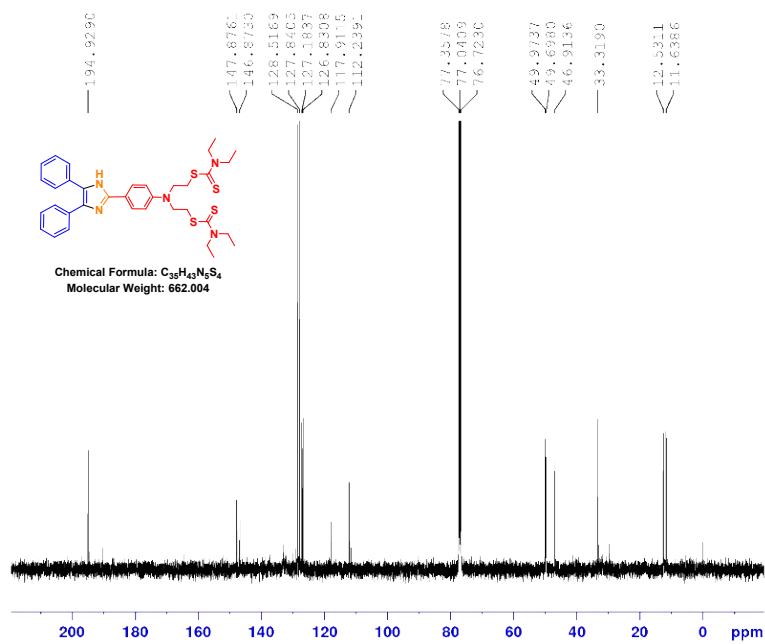


Fig.S5. The ^{13}C NMR spectra of DPICDT.

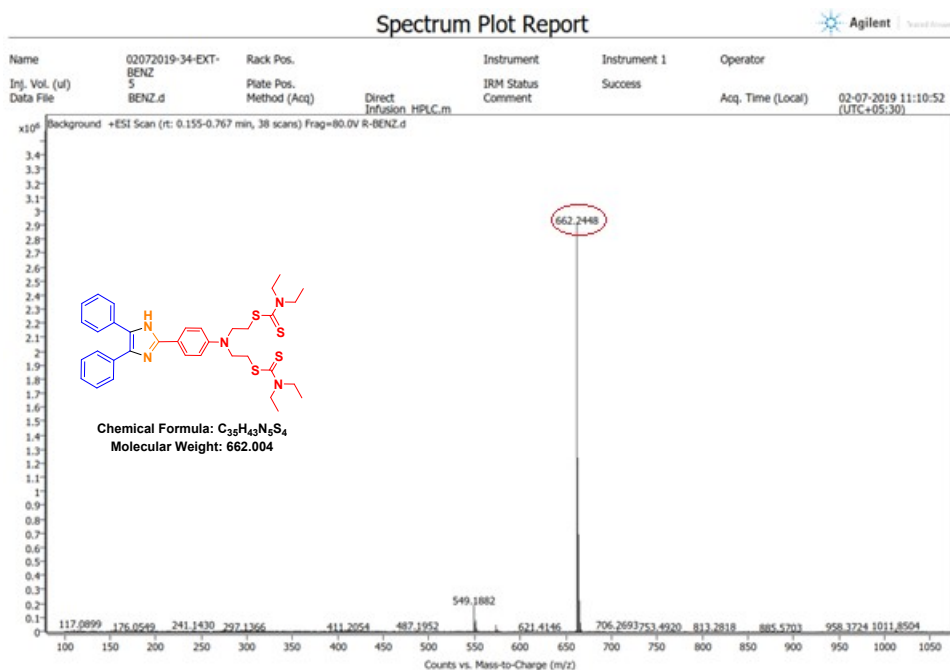


Fig.S6. The HR-MS spectra of DPICDT.

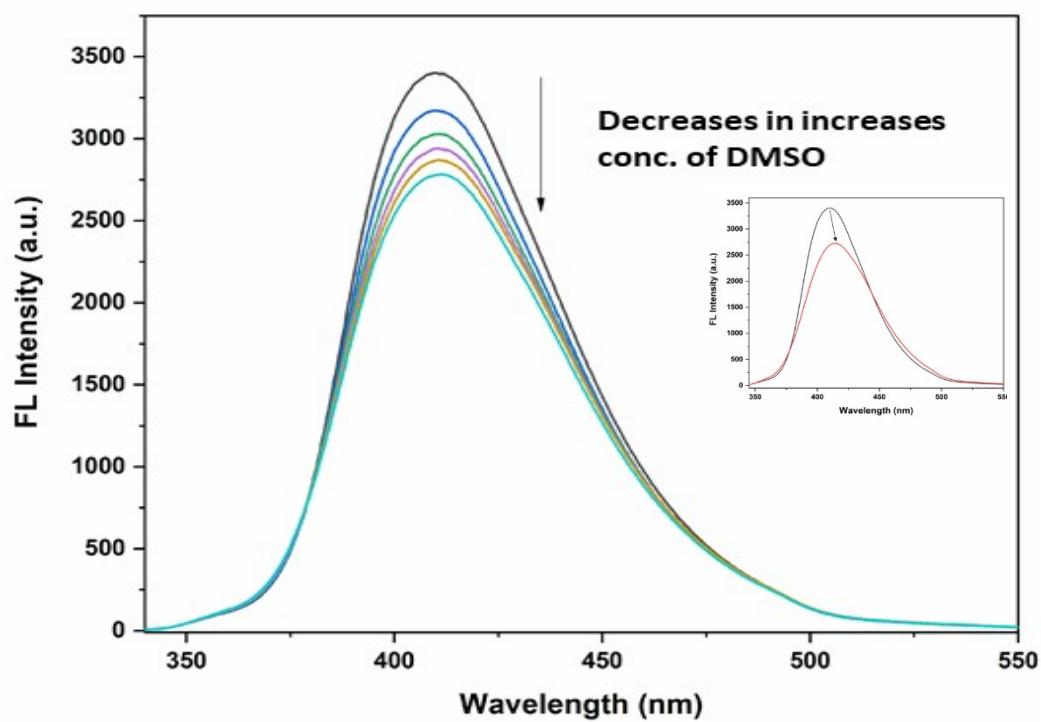


Fig.S7. Changes in fluorescence intensity of DPICDT in THF on the addition of DMSO.

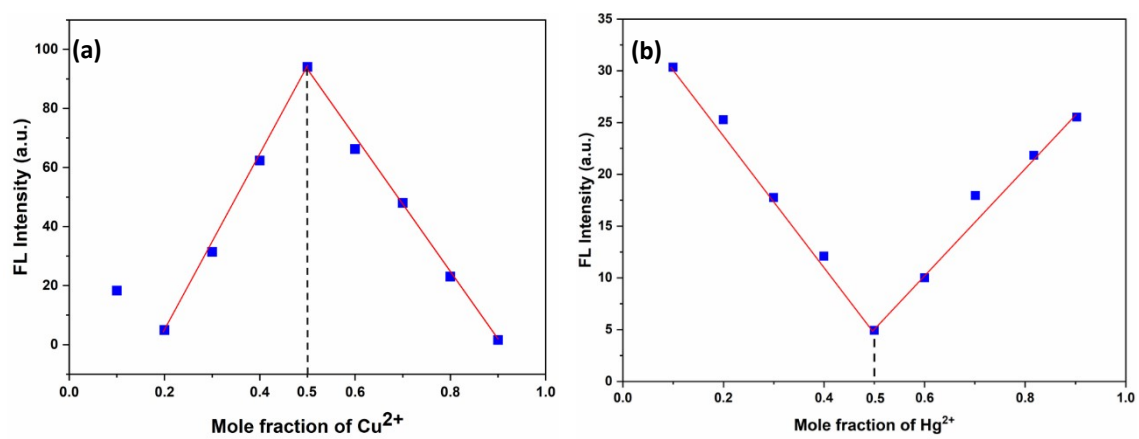


Fig. S8. Job's plot for DPICDT Vs Cu^{2+} (a) and DPICDT Vs Hg^{2+} (b) in $\text{CH}_3\text{CN}:\text{H}_2\text{O}$ (8:2, v/v).

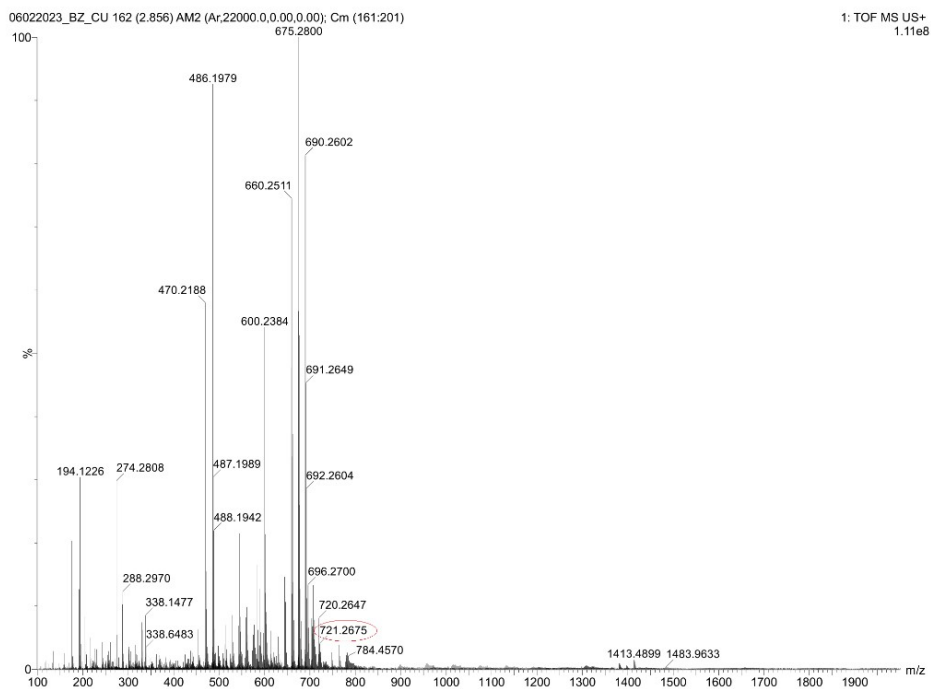


Fig.S9. The HR-MS spectra of DPICDT-Cu²⁺

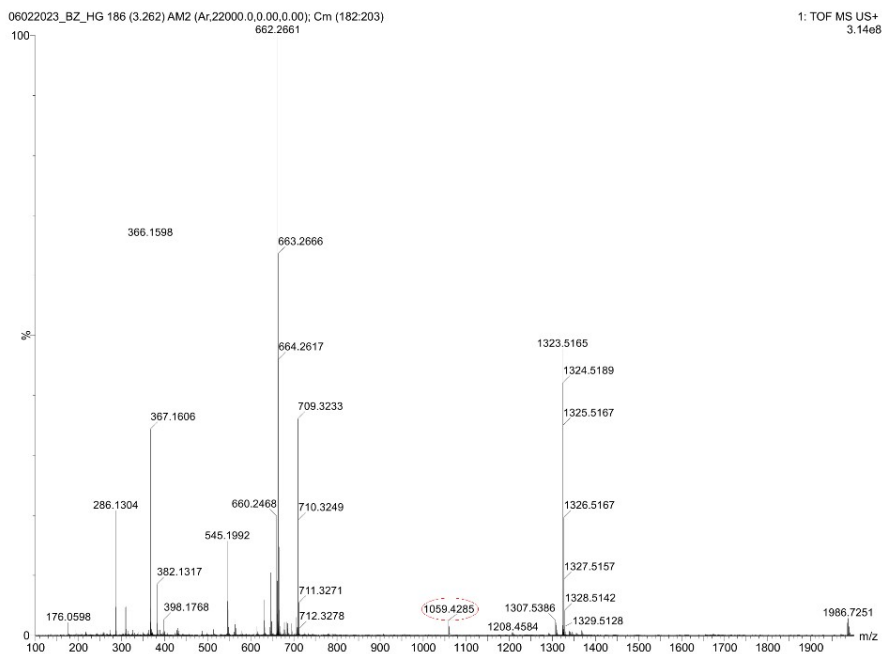


Fig.S10. The HR-MS spectra of DPICDT-Hg²⁺

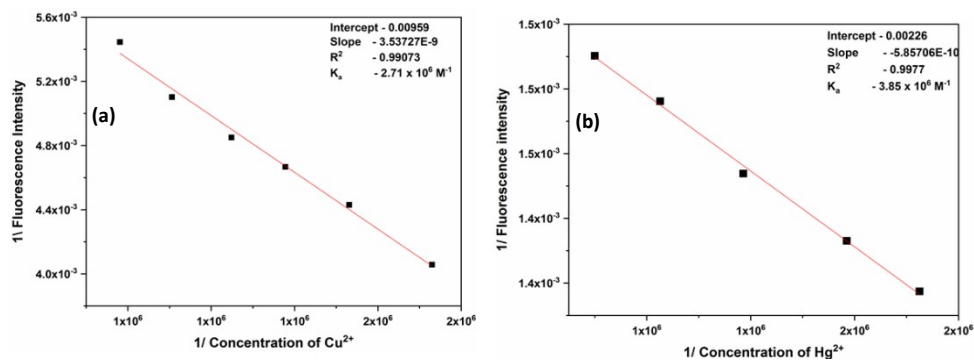


Fig. S11. (a) B–H plot of the 1: 1 complex of probe DPICDT and Cu^{2+} ions (b) B–H plot of the 1: 1 complex of probe DPICDT and Hg^{2+} ions.

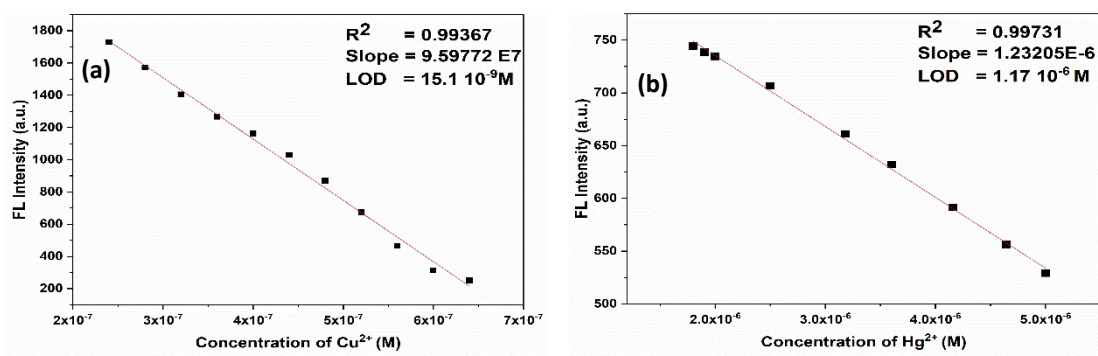


Fig. S12. (a) Linear plot of fluorescence intensity versus concentration of Cu^{2+} ions (b) Linear plot of fluorescence intensity versus concentration of Hg^{2+} ions

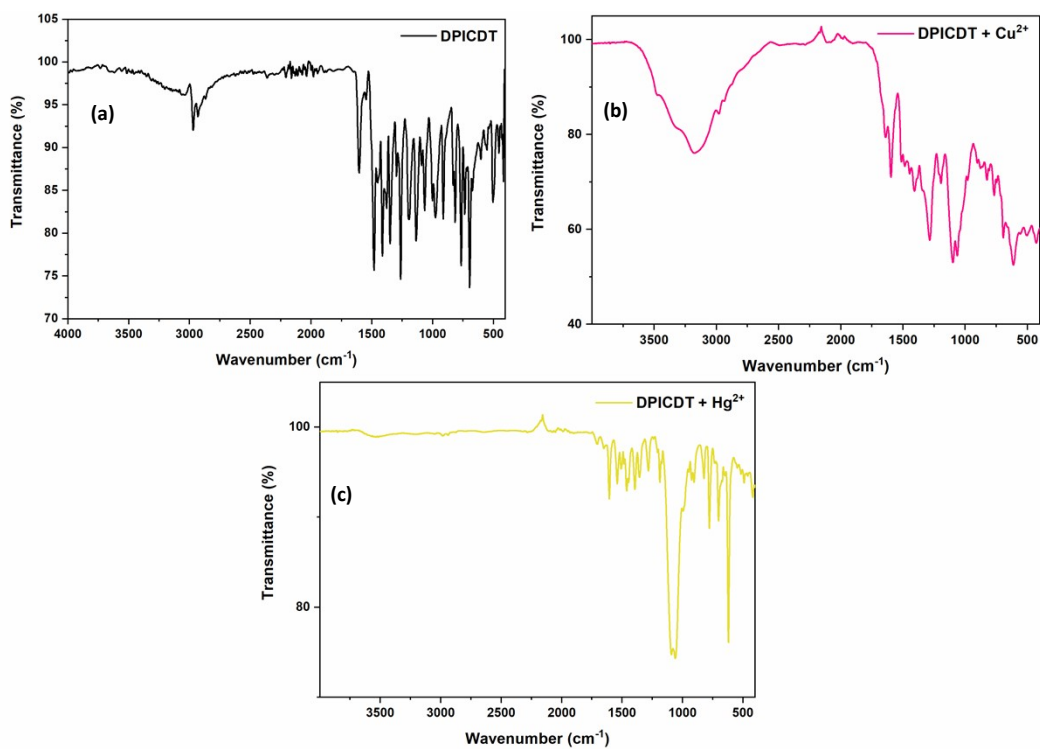


Fig. S13. (a) FT-IR spectra of probe DPICDT (b) DPICDT + Cu²⁺ (c) DPICDT + Hg²⁺

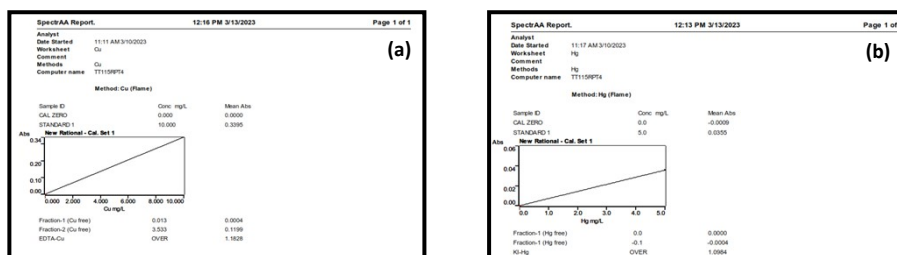


Fig. S14. (a) AAS spectrum calibration plot of the DPICDT with Cu²⁺ (b) DPICDT with Hg²⁺

Table-S1**Recent literature reports on copper.**

S.No	Various substituted core	LOD	Solvent system used	Reversibility	Paper strip studies	Metal extraction	Ref.
1	Schiff-base-based sensor	0.62 μ M	50% ethanol/tris-HCl buffer solution (pH = 7.40)	Done	Done	-	1
2	Naphthaldehyde-pyridoxal based sensor	32.9 nM	DMSO/HEPES (pH = 7.40)	Done	Done	-	2
3	Pyridine-2,6-dicarboxamide-based sensor	1.49 μ M	Pure CH ₃ CN	Done	-	-	3
4	Diaminebenzene-based sensor	15 nM	Pure CH ₃ CN	-	-	-	4
5	1,5-Dihydroxyanthraquinone-based sensor	10 nM	Ethanol	Done	-	-	5
6	Schiffbase-based sensor	1.8 μ M	Methanol - tris-HCl buffer	Done	-	-	6
7	1,8-naphthalimide sensor	17 nM	(CH ₃ CN: H ₂ O) (9.7:0.3) (v\v)	-	-	-	7
8	Triphenylamine benzothiazole-based sensor	0.45 μ M	Pure CH ₃ CN	-	Done	-	8
9	DPICDT (Present work)	15.1 nM	(CH₃CN: H₂O) (8:2) (v\v)	Done	Done	Done	

Table-S2

Recent literature reports of mercury.

S.No	Various substituted core	LOD	Solvent system used	Reversibility	Paper strip studies	Extraction of metals	Ref.
1	Naphthalene based sensor	4.92 μ M	DMSO/buffer (99/1, v/v)	-	-	-	9
2	Chitosan-BODIPY-based sensor	1.51 μ M	Aqueous acetic acid	-	-	-	10
3	Rhodamine-based sensor	3.36 μ M	CH ₃ CN/H ₂ O (v/v:9/1 with HEPES buffer)	-	-	-	11
4	Dipicolylaminoquinoline based sensor	1.01 μ M	NaOAc-AcOH buffer pH = 5.9	Done	-	-	12
5	Squaraine-bis(Rhodamine-B)-based sensor	6.48 μ M	CH ₃ CN	Done	-	-	13
6	Naphthalimide based sensor	2.0 μ M	Tris-HCl buffer (ethanol/water = 1:1, v/v, pH 7.01)	Done	-	-	14
7	DPICDT (Present work)	1.17 μM	(CH₃CN: H₂O) (8:2) (v\ v)	Done	Done	Done	

References

- 1 H. Liu, S. Ding, Q. Lu, Y. Jian, G. Wei and Z. Yuan, 2022, ACS omega, 7, 7585-7594.
- 2 V. Bhardwaj, S.A. Kumar and S.K. Sahoo, 2022, Microchem. J., 178,107404.
- 3 H. Rahimi, R. Hosseinzadeh and M. Tajbakhsh, 2022, J. Photochem. Photobiol. A, 407, 113049.
- 4 A. Kuwar, R. Patil, A. Singh, S.K. Sahoo, J. Marek and N. Singh, 2015, J. Mater. Chem. C., 3, 453-460.
- 5 S. Mohandoss, J. Sivakamavalli, B. Vaseeharan and T. Stalin, 2016, Sens. Actuators B Chem., 234, 300-315.
- 6 A.K. Manna, M. Sahu, K. Rout, U.K. Das and G.K. Patra, 2020, Microchem. J., 157, 104860.
- 7 S.N.K. Elmas, F.N. Arslan and D. Aydin, 2022, Analyst., 147, 2687-2695.
- 8 D. Li, A. Liu, Y. Xing, Z. Li, Y. Luo, S. Zhao, L. Dong, T. Xie, K. Guo and J. Li, 2023, Dyes Pigm., 213, 111180.
- 9 H. Kim, M. Lee, J.J. Lee, E.K. Min, K.T. Kim and C. Kim, 2022, J. Photochem. Photobiol. A., 428, 113882.
- 10 D. Wang, L. Marin and X. Cheng, 2022 Int. J. Biol. Macromol., 198, 194-203.
- 11 S. Bayindir, 2019, J. Photochem. Photobiol. A, 372, 235-244.
- 12 W. Paisuwan, P. Rashatasakhon, V. Ruangpornvisuti, M. Sukwattanasinitt, and A. Ajavakom, 2019, Sens. Bio-Sens., 24, 100283.
- 13 S. Lee, B.A. Rao and Y.A. Son, 2015, Sens. Actuators B Chem., 210, 519-532.
- 14 X.F. Wu, Q.J. Ma, X.J. Wei, Y.M. Hou and X. Zhu, 2013, Sens. Actuators B Chem., 183, 565-573.